KONDRATIEV, A. and JAK, E. Quasi-chemical viscosity model for fully liquid slags in the $A1_2O_3$-CaO-'FeO'-SiO_2 system. *VII International Conference on Molten Slags Fluxes and Salts,* The South African Institute of Mining and Metallurgy, 2004.

Quasi-chemical viscosity model for fully liquid slags in the $A1_2O_3$-CaO- 'FeO'-SiO_2 system

A. KONDRATIEV and E. JAK

PYROSEARCH, Division of Mining and Minerals Process Engineering, The University of Queensland, Brisbane, Australia

A structurally-based viscosity model for fully liquid silicate slags has been developed and applied to the Al_2O_3-CaO-'FeO'-SiO_2 system at metallic iron saturation. The model links the slag viscosity to the internal structure of melts through second nearest neighbour bonds concentrations taken from the quasi-chemical thermodynamic model. This viscosity model describes experimental data over the whole temperature and composition ranges within the Al_2O_3-CaO-'FeO'-SiO_2 system at metallic iron saturation and can now be applied to other industrial slag systems.

Introduction

Development of a reliable and general model that would enable the viscosities of multi-component slag systems to be predicted over a wide range of compositions and temperatures is important for a number of industrial processes. Previously proposed slag viscosity models have recently been reviewed[1-4]. Most of the models are applicable to relatively limited composition and temperature ranges. In the present paper a general, structurally-based viscosity model for fully liquid silicate slags is developed and applied to the pseudo-quaternary Al_2O_3-CaO-'FeO'-SiO_2 system in equilibrium with metallic iron.

Model description

Frenkel's theory of liquids[5-7] considers a liquid far from its critical point to possess a solid-like structure with molecules (or more generally, structural units) oscillating about near average positions in their energetic cells (potential wells)[7]. Higher oscillations result in the movement of a structural unit (SU) into an adjacent cell, provided the latter is vacant. These vacant cells, or holes, are formed in the liquid as a result of fluctuations in short range order or defects inherited from crystal structure, and are distributed randomly in the liquid.

If a shear force is applied to the liquid, the structural units will move not randomly, but preferentially in the direction of the applied force. From this point of view, the viscosity of liquid (reciprocal to its fluidity) as a reaction to the applied shear force is determined by two factors: the ability of structural units to jump over the potential barrier and the presence of holes in the liquid. Frenkel[7] highlighted that in the general case of complex ionic solution, the height of potential barrier, which is related to the activation energy, depends on 'the mutual action of the ions of each sign both on each other and on the ions of the opposite sign'[7], i.e. on the character and quantitative effect of interactions between different ions that make up the liquid. The concentration of holes in a liquid is related to the energy of hole formation[7].

Based on the same postulates of liquid state and liquid viscosity initially formulated by Frenkel[5-7], the Weymann-Frenkel[8] and Eyring[9-11] viscosity equations were derived. The Eyring approach has also been successfully applied to description of other kinetic processes, e.g. diffusion and chemical reactions[9], and has been selected to describe the viscosities of liquid slag systems in the present work.

Viscous flow in Eyring theory[10-11] is considered to be a thermally activated kinetic process in which the structural unit (SU) (atom or molecule in simple liquids) goes from one equilibrium position to another, jumping over a potential barrier. Considering two layers of structural units, one sliding past the other under the influence of an applied shear force and taking certain assumptions, the following equation was derived[9] to describe the viscosities of liquid:

$$\eta = \frac{2RT}{\Delta E_{vap}} \frac{\left(2\pi m_{SU} kT\right)^{1/2}}{v_{SU}^{2/3}} \exp\left(\frac{E_a}{RT}\right), \qquad [1]$$

where R is the gas constant, k is the Boltzmann constant, T is the absolute temperature, ΔE_{vap} is the energy of vaporization, E_a is the activation energy, and m_{SU} and v_{SU} are the weight and volume of the structural unit. The activation energy E_a is related to the potential barrier that has to be overcome by a structural unit to move to the available hole. The energy of vaporization ΔE_{vap}, which was also called by Bockris[12] 'work of hole formation', is closely related to the probability of the formation of a hole, or a free volume in the liquid[9]. For simple liquids, the energy of vaporization can be approximately expressed through the latent heat of vaporization[11]. The Eyring equation has successfully been applied to describe viscosities of liquid silicates[13,14].

The Equation [1] requires the definition of a structural unit and contains four parameters affected by this definition: weight and volume of SU, activation energy, and energy of vaporization. These parameters are clearly related to the internal structure of liquids, the types of structural units and the interactions between them. Silicate slags are

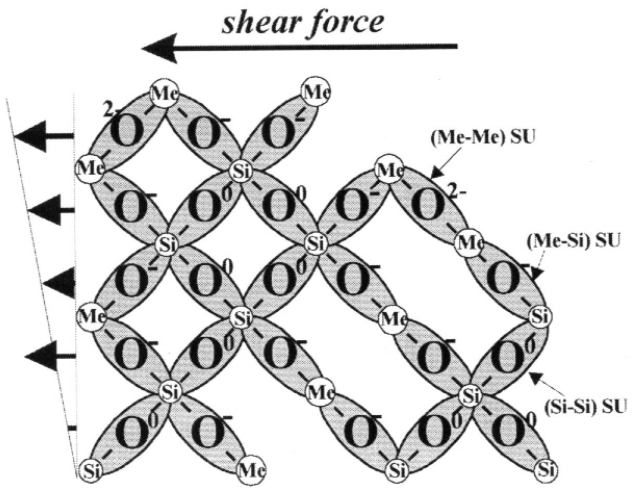

Figure 1. Schematic view of the internal structure and viscous flow in silicate melts. O^0, 0, and 0^{2-}, and O—non-bridging, bridging, and free oxygens, respectively. SU = structural unit

known to have complex internal structures; these should be taken into account in defining the structural units participating in the viscous flow, describing their interactions as a function of their concentrations, and in their incorporation into the viscosity model (Equation [1]).

Definition of structural units

It has been proven that silicate slags possess complex internal structures determined by composition and temperature[15-17]. A silicate slag may be assumed to consist of nearly close-packed arrangements of oxygen anions with smaller metal cations occupying the interstices; these anions and cations interact to form ionic bonds[15]. Fincham and Richardson[18] suggested a silicate slag can be considered to consist of three types of oxygens: 'bridging' (O^0—connected to two silicon cations); 'non-bridging' (O^-–connected to only one silicon); and 'free' (O^{2-}–associated with non-silicon cations). This concept has been successfully used in numerous models related to the silicate slag structure. Figure 1 gives a simplified two-dimensional picture of the internal structure of the binary slag system MeO-SiO_2 that follows from the Fincham-Richardson concept.

From the theoretical description of the viscous flow[7,9] and from the existing interpretation of the internal structure of the slags[18] it can be suggested that viscous flow of the silicate slag may be viewed as a movement of oxygens together with metal cations associated with them, under a shear force applied (see Figure 1). Based on this view it is proposed that the structural units for the silicate slag viscous flow description can be defined as oxygen anions with metal cations partly associated with them. The structural units defined this way are indicated in Figure 1 by shaded areas.

There are clearly a number of different types of structural units that involve oxygen associated with various combinations of metal cations. For example, for the binary MeO-SiO_2 silicate slag (see Figure 1) three types of structural units can be identified (Si-Si), (Me-Si) and (Me-Me); and their concentrations will be indicated as $X_{Si\text{-}Si}$, $X_{Me\text{-}Si}$ and $X_{Me\text{-}Me}$.

Linkage to the quasi-chemical thermodynamic model

In order to describe viscosity according to Equation [1], the mass and volume of the structural units should be defined, the energy of vaporization ΔE_{vap} and the activation energy E_a should be expressed as a function of various SU concentrations. Analysis of Figure 1 clearly indicates that the concentrations of the structural units are equivalent to the concentrations of the bridging O^0, non-bridging O^- and free O^{2-} oxygens identified by the Fincham-Richardson concept[18]. They are also equivalent to the concentrations of the 'structural cells' of the cell thermodynamic model[19].

In the present work the concentrations of structural units are determined using the quasi-chemical thermodynamic (QC) model of the slag, which was developed by Guggenheim[20] and was then further modified by Blander and Pelton[21]. The QC model takes into account short-range ordering of second-nearest-neighbour-cations in the ionic melt. For a binary MeO-SiO_2 slag the quasi-chemical model considers the formation of two nearest-neighbour pairs (Me-Si) from a (Me-Me) and a (Si-Si) pair, which are also called 'second nearest neighbour bonds' (SNNB)[21]. The SNNB molar fractions X_{SNNB} are calculated within the thermodynamic model. Figure 1 illustrates for the binary MeO-SiO_2 system that various types of the proposed structural units participating in the viscous flow are equivalent to the SNN bonds used in the quasi-chemical thermodynamic model. It is clear that the concentrations of these structural units are equal to the concentrations of the corresponding second nearest neighbour bonds of the quasi-chemical thermodynamic model[21].

Since its development, the quasi-chemical model as part of the FactSage (earlier F*A*C*T) computer package[22] has been successfully applied to describe experimental data in many slag systems, from binary to multi-component systems. The concentrations of SNN bonds obtained from the quasi-chemical thermodynamic model are taken as reasonable approximations of the slag internal structures and are used to determine the SU concentrations participating in the viscous flow. In the present study the thermodynamic database for the five-component system Al-Ca-Fe-O-Si developed by one of the authors[23] in collaboration with the FactSage group is used.

Weight and volume of structural units

The average molecular weight m_{SU} and average volume v_{SU} of structural units in the binary MeO-SiO_2 system can be expressed through the concentrations of different structural units present in the melt in the following form:

$$m_{SU} = m_{Si-Si}X_{Si-Si} + m_{Me-Si}X_{Me-Si} + m_{Me-Me}X_{Me-Me}, \quad [2]$$

$$v_{SU} = v_{Si-Si}X_{Si-Si} + v_{Me-Si}X_{Me-Si} + v_{Me-Me}X_{Me-Me}, \quad [3]$$

where $m_{Si\text{-}Si}$, $v_{Si\text{-}Si}$ and $X_{Si\text{-}Si}$; $m_{Me\text{-}Si}$, $v_{Me\text{-}Si}$, and $X_{Me\text{-}Si}$; and $m_{Me\text{-}Me}$, $v_{Me\text{-}Me}$ and $X_{Me\text{-}Me}$ are the weights, volumes and the molar fractions of the (Si-Si), (Me-Si), and (Me-Me) structural units, respectively. Weights $m_{Si\text{-}Si}$, $m_{Me\text{-}Me}$ and $m_{Me\text{-}Si}$ are equal to the weights of single molecules of the liquid $Si_{0.5}O$, $Me^{n+}{}_{2/n}O$ and $Me^{n+}{}_{1/n}Si_{0.25}O$ respectively, where n is the oxidation state of a metal cation Me^{n+}. It was assumed that the volumes of the structural units are independent of composition; thus, $v_{Si\text{-}Si}$ and $v_{Me\text{-}Me}$ are equal to the volumes of single 'molecules' of the liquid $Si_{0.5}O$ and

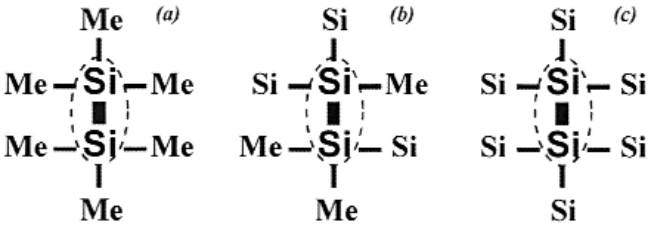

Figure 2. Examples of different nearest neighbours of a given (Si-Si) structural unit

$Me^{n+}_{2/n}O$, respectively. The experimental data on the densities of the corresponding liquid orthosilicates[22,24] have been used to calculate $v_{Me\text{-}Si}$. If no experimental data have been found, a linear approximation between pure components was used to estimate these values. It has also been assumed that the volumes of the structural units do not change with temperature. Average uncertainty in density value caused by these assumptions is estimated for some binary systems to be approximately ±5%. The effect of this uncertainty on the slag viscosity does not exceed ±3%; and is 1% on average for most of the slags and is compensated for by other parameters.

Activation and vaporization energies

As it was quoted above, according to Frenkel, the activation energy of viscous flow (or the height of potential barrier) and the concentration of holes in a liquid (or the energy of hole formation) in complex ionic solutions are determined by mutual interaction between the various types of structural units[7]. The overall integral molar activation energy can then be assumed to be proportional to the partial molar activation energies and concentrations of each type of SU. Thus, in the binary system MeO-SiO_2 the molar activation energy can be expressed as follows:

$$E_a = E_{a,Si-Si}X_{Si-Si} + E_{a,Me-Si}X_{Me-Si} + E_{a,Me-Me}X_{Me-Me}, \quad [4]$$

where $E_{a,Si\text{-}Si}$, $E_{a,Me\text{-}Si}$ and $E_{a,Me\text{-}Me}$ are the partial molar activation energies and $X_{Si\text{-}Si}$, $X_{Me\text{-}Si}$ and $X_{Me\text{-}Me}$ are the molar fractions of each type of SU, respectively.

A given structural unit involves one oxygen and two metal cations. Each of these two metal cations in turn has other neighbours and is involved in other structural unit(s). The forces holding the first considered SU (and therefore corresponding partial molar activation energy) are assumed to depend on other neighbours each of these two metal cations have. For example, if the two Si cations forming a (Si-Si) structural unit have other metal cation neighbours (Figure 2a), they will have a different partial activation molar energy compared to a case when some or all other neighbours are also silicon ions (Figures 2b and 2c). The effects of neighbouring structural units on a partial activation energy is assumed to be dependent on the concentrations of the other types of structural units, so the partial molar activation energy of each type of SU in the Equation [4] can be calculated as follows:

$$E_{a,Si-Si} = E^0_{a,Si-Si} + E^{Si-Si,1}_{a,Si-Si}X_{Si-Si} + E^{Si-Si,2}_{a,Si-Si}X^2_{Si-Si} + E^{Me-Si}_{a,Si-Si}X_{Me-Si}, \quad [5]$$

$$E_{a,Me-Si} = E^0_{a,Me-Si} + E^{Me-Si}_{a,Me-Si}X_{Me-Si} + E^{Si-Si}_{a,Me-Si}X_{Si-Si} + E^{Me-Me}_{a,Me-Si}X_{Me-Me}, \quad [6]$$

$$E_{a,Me-Me} = E^0_{a,Me-Me} + E^{Me-Me}_{a,Me-Me}X_{Me-Me} + E^{Me-Si}_{a,Me-Me}X_{Me-Si}. \quad [7]$$

To satisfactorily describe the experimental data in the binary silicates it was necessary to introduce a term in $X^2_{Si\text{-}Si}$.

Extensive analysis of the experimental data for a number of silicate systems indicated that adequate description of ΔE_{vap} as a function of X_{SU} can be achieved in the following form (for the binary system MeO-SiO_2):

$$\Delta E_{vap} = \exp\left(E_{v,Si-Si}X_{Si-Si} + E_{v,Me-Si}X_{Me-Si} + E_{v,Me-Me}X_{Me-Me}\right), \quad [8]$$

where $E_{v,Si\text{-}Si}$, $E_{v,Me\text{-}Si}$ and $E_{v,Me\text{-}Me}$ are the partial vaporization energies of each type of a structural unit, and $X_{Si\text{-}Si}$, $X_{Me\text{-}Si}$ and $X_{Me\text{-}Me}$ are the molar fractions of corresponding types of structural units.

Charge compensation effect

It has been found experimentally[16] that Al^{3+} can replace Si^{4+} in tetrahedral coordination positions if the excess negative charge for Al^{3+} is compensated by the presence of alkali or alkaline earth cations, thus keeping the silicate network structure instead of breaking it. As a result, associates of the form $Me^{+}AlO_2$ or $Me^{2+}Al_2O_4$ are formed in the melt. This is commonly referred to as the 'charge compensation effect'[16]. A number of experimental studies in the Al_2O_3-(Me_2,Me)O-SiO_2 systems[3,16] also reported behaviour of viscosity as a function of composition, which can be attributed to the charge compensation effect[25]. For example, in the Al_2O_3-CaO-SiO_2 system the viscosity was reported to have a maximum at $X_{CaO}/X_{Al_2O_3} \approx 1$[26,27]. The same phenomenon was observed in other Al_2O_3-(Na_2, K_2, Mg)O-SiO_2 systems[3]. The current quasi-chemical model does not describe the charge compensation effect[28]. In order to describe the viscosity behaviour in the Al_2O_3-(Ca, Fe)O-SiO_2 systems, the following charge compensation term therefore is added to the activation energy of viscous flow:

$$E^{ch/c}_a = E^{ch/c}_{a\_AlMe}\left(2X_{Al-Al} + X_{Al-Si}X_{Al-Me}\right)^{\alpha}\left(2X_{Me-Me} + X_{Me-Si} + X_{Al-Me}\right)^{\beta}X_{Si-Si}, \quad [9]$$

where $E^{ch/c}_{a\_AlMe}$, α, and β are adjustable parameters. A reasonable description of viscosity in the Al_2O_3-CaO-SiO_2 system was achieved with only these three additional parameters. The charge compensation term $E^{ch/c}_a$ (Equation [9]) is proportional to the concentrations of Al^{3+} and (Me^{+} or Me^{2+}) cations in the melt (first and second brackets, respectively). Values α and β were optimized to achieve the maximum of the charge compensation term at $X_{CaO}/X_{Al_2O_3} \approx 1$ to ensure the best agreement with the experimental data. $E^{ch/c}_a$ is also proportional to the concentration of (Si-Si) structural units, reflecting the fact that the charge compensation effect appears only in the presence of the silicate network.

Experimental data

The review and selection of most of the available experimental sources of viscosity data for the Al_2O_3-CaO-

'FeO'-SiO_2 system in equilibrium with metallic iron (including all its sub-systems) have recently been described by the authors in detail elsewhere[29]; a few additional studies[30-37] have also been reviewed and some of them used in the present work. Altogether approximately 4 700 experimental points for the four-component system Al_2O_3-CaO-'FeO'-SiO_2 have been critically analysed.

Experimental measurements of slag viscosities at high temperatures are subject to a number of error sources. Aggressive molten slags may dissolve container and sensor materials, resulting in changes of slag composition and of container/sensor geometry. Post-experimental analysis of the slag compositions reduces these potential errors. Temperature control using a thermocouple adjacent to the sample has better precision compared to an optical pyrometer. Measurements in the iron oxide-containing slag systems require either oxygen partial pressure P_{O2} control or use of the metallic iron crucibles. The rotating bob/crucible method is considered by many authors[38] to be a more accurate and reliable technique for the high temperature viscosity measurements compared to other methods including Shvidkovski method and vibrational viscometer. These and other considerations were used in the critical review of the data and the selection of data for the development of the model. Over 3 700 experimental points were selected for the optimization in total.

Optimization procedure

The mass and volume of each of the structural units were determined first using available density data. A viscosity value at a given composition then is dependent on two parameters—ΔE_{vap} and E_a. The same viscosity can be obtained with different values of ΔE_{vap} and E_a in case there is no other constraint, i.e. temperature dependency information for a given composition. This factor was taken into account and the parameters for the viscosity model were optimized in two steps: (1) the 'experimental' activation and vaporization energies were found for those experimental points with the available temperature dependence at a given composition; (2) the calculated viscosities were then fitted into all other accepted experimental values over the whole composition range in the four-component system Al_2O_3-CaO-'FeO'-SiO_2. 'Experimental' values for the activation and vaporization energies in the first stage of optimization were found using Equation [1] by fitting into experimental viscosities at each

$$m_{SU}\left[10^{-26}kg\right] = 4.99X_{Si-Si} + 5.64X_{Al-Al} + 9.31X_{Ca-Ca} + 11.93X_{Fe-Fe} + 5.32X_{Al-Si} + 7.15X_{Ca-Si}$$
$$+8.46X_{Fe-Si} + 7.48X_{Al-Ca} + 8.79X_{Al-Fe} + 10.62X_{Ca-Fe}; \quad [10]$$

$$v_{SU}\left[10^{-29}m^3\right] = 2.49X_{Si-Si} + 1.88X_{Al-Al} + 2.78X_{Ca-Ca} + 2.03X_{Fe-Fe} + 2.13X_{Al-Si} + 2.67X_{Ca-Si}$$
$$+2.82X_{Fe-Si} + 2.99X_{Al-Ca} + 3.51X_{Al-Fe} + 4.25X_{Ca-Fe}; \quad [11]$$

$$E_a\left[10^2 kJ/mol\right] = E_{a,Si-Si}X_{Si-Si} + E_{a,Al-Al}X_{Al-Al} + E_{a,Ca-Ca}X_{Ca-Ca} + E_{a,Fe-Fe}X_{Fe-Fe} + E_{a,Al-Si}X_{Al-Si}$$
$$+E_{a,Ca-Si}X_{Ca-Si} + E_{a,Fe-Si}X_{Fe-Si} + E_{a,Al-Ca}X_{Al-Ca} + E_{a,Al-Fe}X_{Al-Fe} + E_{a,Ca-Fe}X_{Ca-Fe} + E_{a,AlCa}^{ch/c} + E_{a,AlFe}^{ch/c}, \ where \quad [12]$$

$$E_{a,Si-Si} = 1.94 - 4.55X_{Si-Si} + 8.06X_{Si-Si}^2 + 7.29X_{Al-Si} + 0.91X_{Ca-Si} + 2.63X_{Fe-Si},$$
$$E_{a,Al-Al} = 1.29 + 0.64X_{Al-Si} + 3.31X_{Al-Ca}0.80X_{Al-Fe},$$
$$E_{a,Ca-Ca} = 0.82 - 1.11X_{Ca-Si} + 1.44X_{Al-Ca} - 0.12X_{Ca-Fe},$$
$$E_{a,Fe-Fe} = 0.50 - 0.25X_{Fe-Si} - 0.58X_{Al-Fe} - 0.09_{Ca-Fe},$$
$$E_{a,Al-Si} = 2.53 - 1.96X_{Al-Si} - 1.58X_{Ca-Si} - 1.50X_{Fe-Si} + 3.15X_{Al-Ca} - 4.90X_{Al-Fe},$$
$$E_{a,Ca-Si} = 2.26 - 1.05X_{Ca-Si} + 1.00X_{Fe-Si} + 0.76X_{Al-Ca} - 1.10X_{Ca-Fe},$$
$$E_{a,Fe-Si} = 0.63 - 0.43X_{Fe-Si} + 1.50X_{Al-Fe} - 3.30X_{Ca-Fe},$$
$$E_{a,Al-Ca} = 0.37 + 1.20X_{Al-Ca} + 1.31X_{Al-Fe} + 0.87X_{Ca-Fe},$$
$$E_{a,Al-Fe} = 1.20 - 0.60X_{Al-Fe} - 0.28X_{Ca-Fe}, E_{a,Ca-Fe} = 0.67 - 0.12X_{Ca=Fe},$$
$$E_{a,AlCa}^{ch/c} = 4.60\ \left(2X_{Al-Al} + X_{Al-Si} + X_{Al-Ca}\right)^{2.36}\left(2X_{Ca-Ca} + X_{Ca-Si} + X_{Al-Ca}\right)^{0.94}X_{Si-Si},$$
$$E_{a,AlFe}^{ch/c} = 2.40\ \left(2X_{Al-Al} + X_{Al-Si} + X_{Al-Fe}\right)^{2.36}\left(2X_{Fe-Fe} + X_{Fe-Si} + X_{Al-Fe}\right)^{0.94}X_{Si-Si};$$

$$\Delta E_{vap}\left[J/mol\right] = \exp(E_{v,Si-Si}X_{Si-Si} + E_{v,Al-Al}X_{Al-Al} + E_{v,Ca-Ca}X_{Ca-Ca} + E_{v,Fe-Fe}X_{Fe-Fe} + E_{v,Al-Si}X_{Al-Si} +$$
$$+E_{v,Ca-Si}X_{Ca-Si} + E_{v,Fe-Si}X_{Fe-Si} + E_{v,Al-Ca}X_{Al-Ca} + E_{v,Al-Fe}X_{Al-Fe} + E_{v,Ca-Fe}X_{Ca-Fe}), \ where \quad [13]$$

$$E_{v,Si-Si} = 27.69 - 19.60X_{Si-Si} + 14.00X_{Si-Si}^2 + 3.22X_{Al-Si} - 6.01X_{Ca-Si} + 0.1X_{Fe-Si},$$
$$E_{v,Al-Al} = 13.93 + 9.02X_{Al-Ca}, E_{v,Ca-Ca} = 13.51,\ E_{v,Fe-Fe} = 11.75,$$
$$E_{v,Al-Si} = 19.15 - 6.03X_{Al-Si} + 0.50X_{Ca-Si} + 9.60X_{Fe-Si} + 18.60X_{Al-Ca},$$
$$E_{v,Ca-Si} = 14.67 + 22.75X_{Fe-Si} - 0.70X_{Al-Ca}, E_{a,Fe-Si} = 9.62 + 0.40X_{Fe-Si} - 5.30X_{Al-Si} + 69.80X_{Ca-Fe},$$
$$E_{a,Al-Ca} = 16.58,\ E_{a,Al-Fe} = 11.37,\ E_{a,Ca-Fe} = 11.39.$$

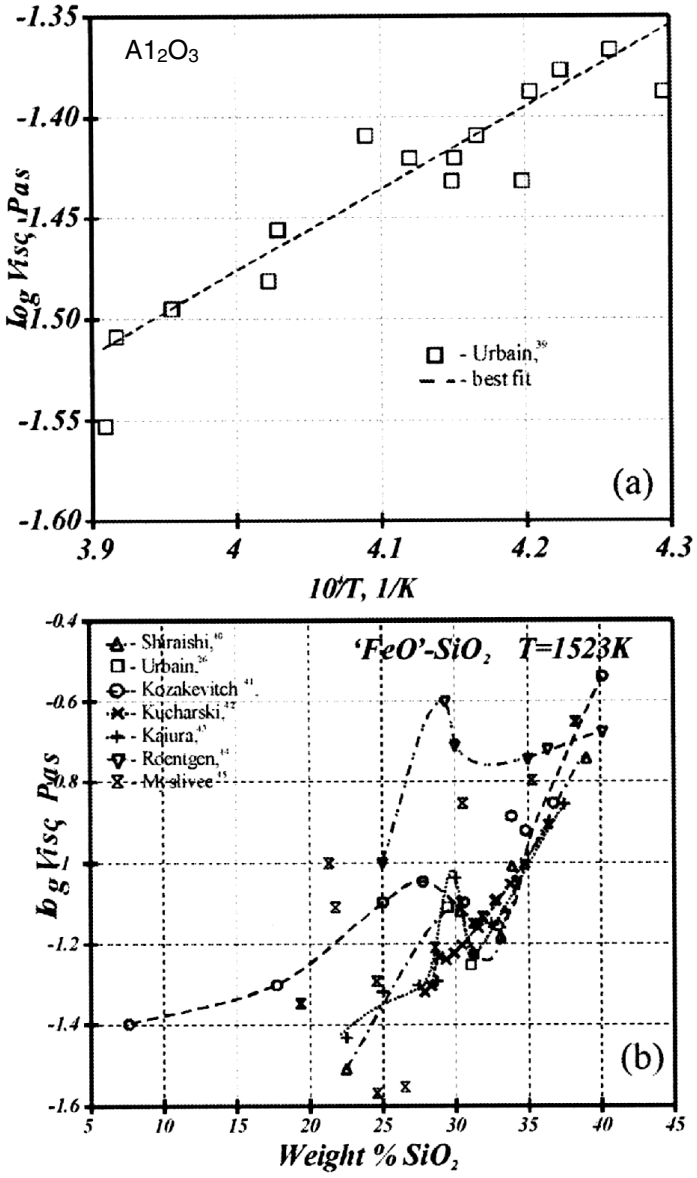

Figure 3. Internal scatter of experimental data: (a) within one dataset, (b) between different datasets

particular composition by adjusting constants E_a and ΔE_{vap}. The 'experimental' values of ΔE_{vap} and E_a obtained in the first step of optimization were also used together with the viscosity values.

After initial parameters, estimation the cycle of parameter adjustment from unary, binary and ternary systems to the quaternary data and back was repeated until satisfactory agreement with all accepted experimental data was achieved. The final set of model parameters therefore describes the experimental viscosities as well as the experimental activation and vaporization energies. The parameters of the quasi-chemical viscosity model for the Al_2O_3-CaO-'FeO'-SiO_2 system at iron saturation are given by Equations [10–13]:

Results and discussion

In assessing the ability of the model to describe the viscosities of slags over a wide range of compositions, temperatures and oxygen pressures, two separate issues should be considered: (1) the inherent scatter in the available data and (2) the description of these data by the model.

Internal scatter is always present within a particular dataset and between different experimental sources (see Figure 3), which we will further refer to as 'internal variability'. The scatter within a given data set (Figure 3a) is usually called 'repeatability'. The scatter between different data sets (Figure 3b) is usually referred to as 'reproducibility'. It can be seen from Figure 3 that the scatter can be very high compared to the experimental uncertainty reported by different authors. It is sometimes possible to reject a particular dataset because of inaccuracies of the experimental technique used (see section 'Experimental data'), but in many cases the internal variability determines the limits of the best agreement achievable in terms of a given viscosity model. The procedure used in the present study to evaluate the internal variability of the experimental dataset in the Al_2O_3-CaO-'FeO'-SiO_2 system at metallic iron saturation is outlined below. First, the following assumptions have been made:

1. Weymann-Frenkel equation[27] for a given composition can perfectly describe temperature dependence of the slag viscosity;
2. Within a narrow composition range the modified Urbain model[29] can perfectly describe compositional dependence of the slag viscosity.

All experimental data for each sub-system have been sub-divided into small compositional areas (within 5 mol pct)

Table I.
Internal variability and model evaluation factor for available systems.

System	Accepted points	Internal variability, %	Model evaluation factor, %	
			modified Urbain model[29]	quasi-chemical viscosity model
Al_2O_3	38	9.6	13.0	10.9
SiO_2	51	9.0	19.1	12.4
Al_2O_3-SiO_2	58	5.3	30.1	12.4
Al_2O_3-CaO	65	10.3	76.0	25.1
CaO-SiO-$_2$	205	7.3	10.9	11.4
Al_2O_3-CaO-SiO_2	597	17.1	31.2	29.7
'FeO'-SiO_2	432	5.0	8.1	6.5
CaO-'FeO'-SiO_2	819	8.4	9.9	10.6
Al_2O_3-CaO-'FeO'	44	12.1	86.6	19.6
Al_2O_3-CaO-'FeO'-SiO_2	1448	21.2	29.2	27.6
Average	**3757**	**10.5**	**31.4**	**16.6**

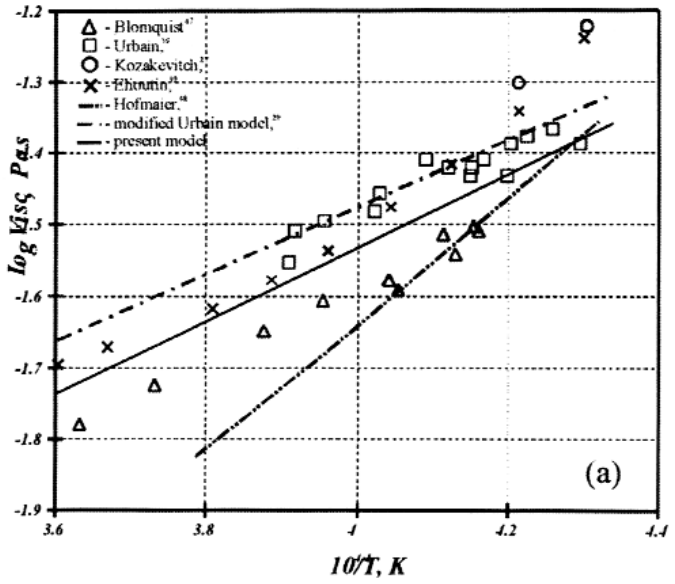

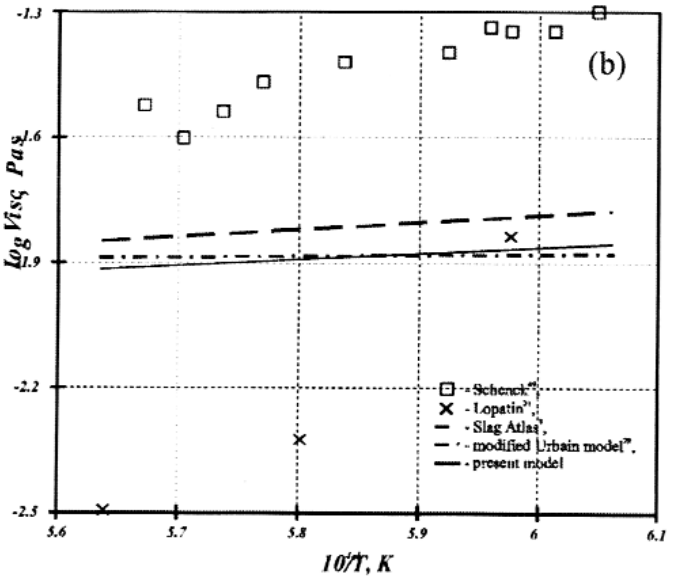

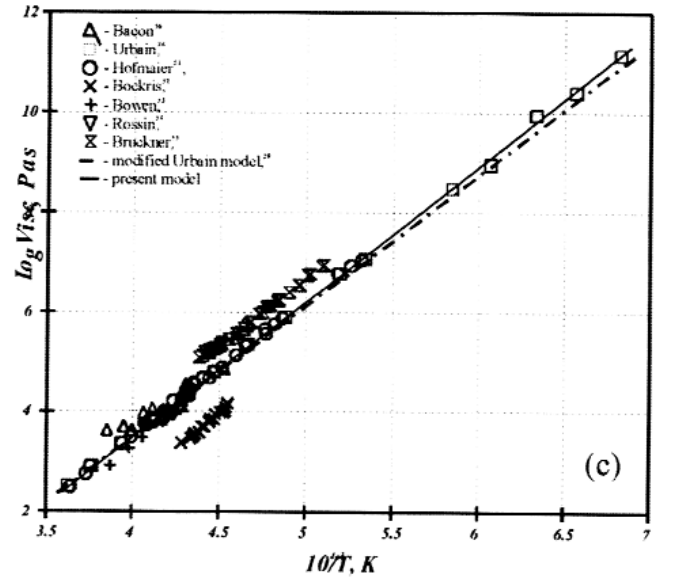

Figure 4. Viscosities of the: (a) pure Al_2O_3; (b) pure 'FeO'; (c) pure SiO_2

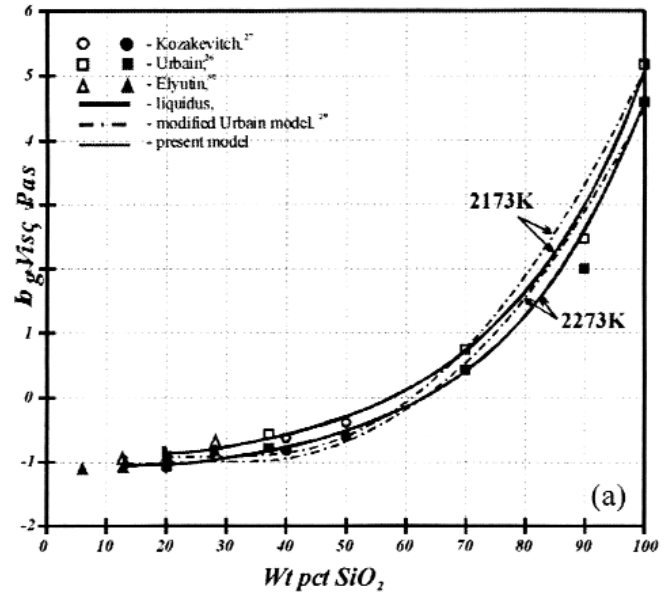

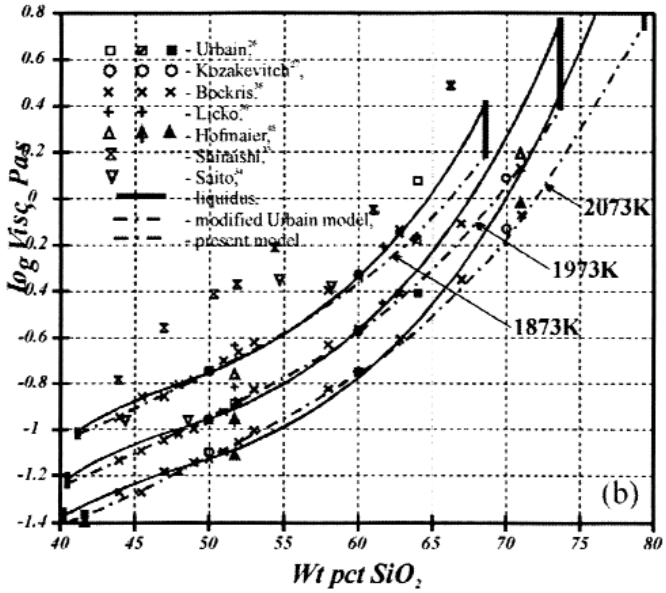

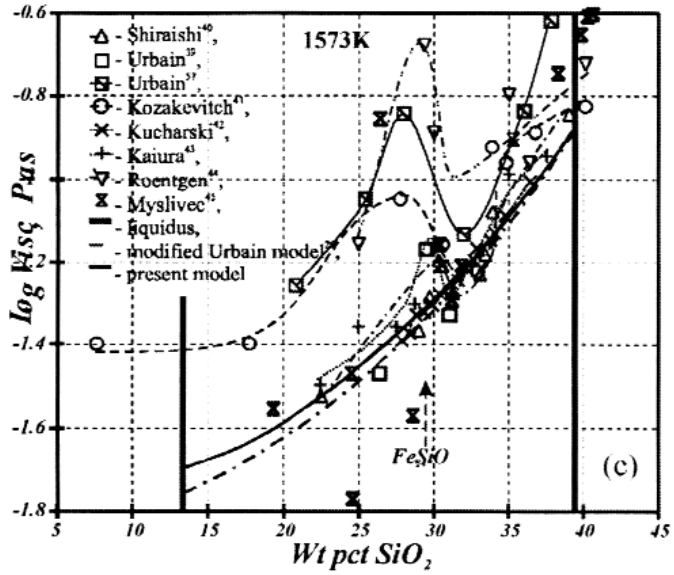

Figure 5. Viscosities of the : (a) Al_2O_3-SiO_2; (b) CaO-SiO_2; (c) 'FeO'-SiO_2

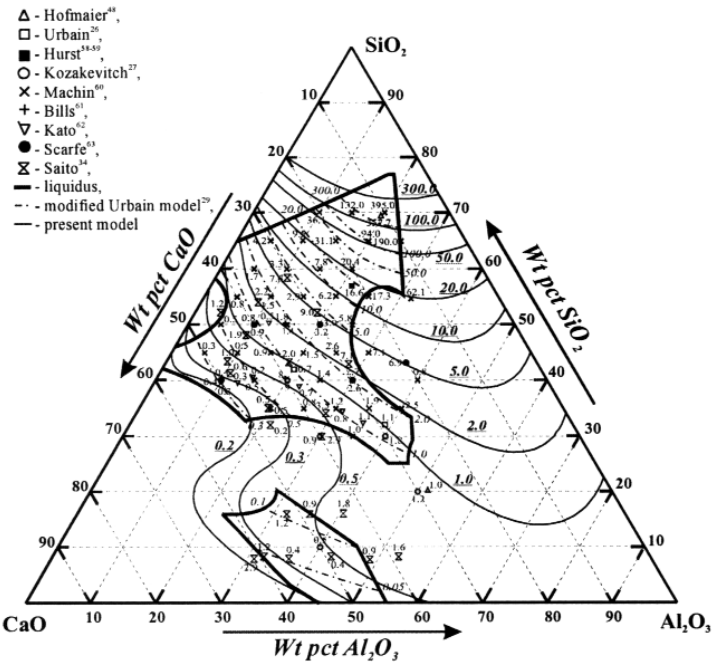

Figure 6. Experimental and calculated viscosities (Pa•S) in the Al_2O_3-CaO-SiO_2, system at 1773K.

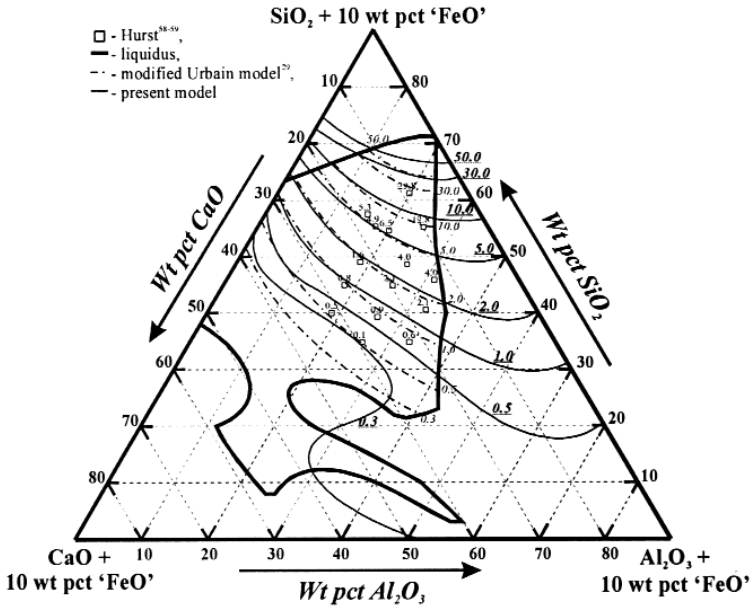

Figure 7. Experimental and calculated viscosities (Pa•S) in the Al_2O_3-CaO-SiO_2, system in equilibrium with metallic iron at 1473K and 'FeO' = 10 wt pct.

and the best fit for each small area was found by adjusting appropriate parameters. Since the compositional areas were so small, the true viscosity values could have been approximated within them with very high precision. The overall deviations from these fits can then be taken as an indicator of the internal variability of experimental data for each sub-system. Table I presents the number of accepted data points, internal variability of these data, and model evaluation factor for each sub-system in the Al_2O_3-CaO-'FeO'-SiO_2 system. Both the internal variability and model evaluation factor were calculated using the formula proposed by Mills *et al.*[46]:

$$\Delta = \frac{1}{N}\sum^{N}\left|\frac{(\eta_n)_{calc} - (\eta_n)_{ex}}{(\eta_n)_{ex}}\right|,$$

where N is a number of points and n is a particular slag system, the subscripts *calc* and ex refer to the calculated and experimental viscosities at a given composition and process condition.

It is clearly seen that the description of the experimental viscosities in the Al_2O_3-CaO-'FeO'-SiO_2 system at metallic iron saturation provided by the quasi-chemical viscosity model is in general better than the modified Urbain model. Significant improvements in description have been achieved in certain systems (e.g. Al_2O_3-SiO_2, Al-$_2O_3$-CaO) as well as for the whole system. The average uncertainty for the quasi-chemical viscosity model assessed by the model evaluation factor for 10 slag systems and over 3 700 experimental points is 16.6 pct, which is almost half that for the modified Urbain model. These values should be compared to and include the 10.5% internal variability of the experimental data set itself.

The following figures present the comparison between the model predictions and experimental data for a few important sub-systems. The modified Urbain model[29] predictions are also shown for comparison. Figure 4a presents the experimental[26,30,39,47,48] and predicted viscosities of the pure Al_2O_3 oxide versus reciprocal temperature. It can be seen from the figure that the predictions of the QC viscosity model are close to the average between all experimental data except Hofmaier[48]. These latter data are rejected due to the obvious inconsistency with the other results. Figure 4b shows the viscosities for the 'FeO' at metallic iron saturation. Both authors[31,49] did not report that the atmosphere was controlled during the experiments. Lopatin *et al.*[31] used molybdenum crucibles, but reported that the slag composition contains 91.5 per cent of FeO. These data therefore can be plotted on the unary graph for comparison. Figure 4b indicates a large discrepancy between these two studies. Predicted viscosities therefore were optimized as close to the recommended by Slag Atlas values[3] as possible. The experimental[26,50-55] and predicted viscosities of the pure SiO_2 are given in Figure 4c. The detailed analysis[29] indicated that the optimization should be based mostly on two consistent studies by Urbain[26] and by Hofmaier[51]. It can be seen from Figure 4c that the present model predictions describe experimental viscosities better than those of the previous model[29].

Figure 5a represents the viscosities of the Al_2O_3-SiO_2 system at 2173 and 2273 K. The present model describes the experimental results[26,27,30] in general better than the modified Urbain model[29]. Agreement between the calculated and experimental viscosities[26,27,33,34,48,56] in the CaO-SiO_2 system at 1873, 1973 and 2073 K is shown at Figure 5b. Results of Shiraishi *et al.*[33] as well as of Saito[34] appeared inconsistent with the other measurements, and therefore were not used in the present optimization. More weight has been given to the data by Urbain[26]. This resulted in a difference between the present model and the modified Urbain model at higher SiO_2 concentrations. Figures 5c presents the experimental[39-45,57] and calculated viscosities in the 'FeO'-SiO_2 system in equilibrium with metallic iron at 1573 K. The priority has been given to the most recent studies[39,42-43].

Good agreement between the model predictions and experimental viscosities[26,27,34,48,58-63] in the Al_2O_3-CaO-SiO_2 system at 1773 K is demonstrated in Figure 6. Results of Saito *et al.*[34] differ significantly from the others and have been rejected. Iso-viscosity curves repeat trends of the iso-SNNB curves. For example, approaching pure CaO the influence of (Ca-Si) structural unit concentrations becomes very strong resulting in 'waves' in viscosity curves at SiO_2 contents less than 40 wt%. This is due to the fact that the present viscosity model is closely related to the slag structure, which in turn is described by the SNNB concentrations. This can be taken as confirmation of the predictive power of the present model.

Figure 7 presents the experimental viscosities[58-59] and calculated isocombs in the Al_2O_3-CaO-'FeO'-SiO_2 system in equilibrium with metallic iron at 1473 K and 10 wt% of 'FeO'. Trends of iso-viscosity curves are very similar to those of the modified Urbain model[29] except in low silica area. Data by Chen *et al.*[36] was not accepted for the optimization due to the inconsistency with the other studies. Sheludyakov *et al.*[37] did not report either the atmosphere of experiments or post-experimental analysis done. These results were also not accepted for the optimization.

Conclusions

A quasi-chemical viscosity model has been developed for liquid slag in the Al_2O_3-CaO-'FeO'-SiO_2 system in equilibrium with metallic iron, this model is directly related to the internal slag structure. The structures of the slags have been determined from the second nearest neighbour bond concentrations extracted from the modified quasi-chemical model available in the FactSage package. The model parameters are valid for the whole range of compositions in the Al_2O_3-CaO-'FeO'-SiO_2 system.

The method of estimating the internal variability of experimental data has been suggested. This method can be used to evaluate the best achievable fit of a viscosity model. The present model has in general a better agreement than the modified Urbain model[29] in the binary systems. The model predicts the slag viscosities reasonably well over the whole composition range in the Al_2O_3-CaO-'FeO'-SiO_2 system at metallic iron saturation. The model can now be extended to other chemical systems and various industrial applications.

Acknowledgements

The authors would like to acknowledge the Australian Research Council for financial support of this project. The authors would also like to acknowledge the significant contribution of Professor Peter C. Hayes to this study and express special thanks to him for valuable discussion and comments.

References

1. KONDRATIEV, A., JAK, E., and HAYES, P.C.: *JOM*, 2002, vol. 54, pp. 41–45.
2. SRIDHAR, S.: *JOM*, 2002, vol. 54, pp. 46–50.
3. MILLS, K.C.: *Slag Atlas*, 1995, chap. 9, pp. 349–402.
4. VARGAS, S., FRANDSEN, F.J., and DAM-JOHANSEN, K.: *Prog. Energy Combust. Sci.*, 2001, vol. 27, pp. 237–429.
5. FRENKEL, J.: *Z. Phys.*, 1926, vol. 35, pp. 652–669.
6. FRENKEL, J.: *Trans. Faraday Soc.*, 1937, vol. 33, pp. 58–65.
7. FRENKEL, J.: *Kinetic theory of liquids*, Oxford University Press, UK, 1946, 488 pp.
8. WEYMANN, H.D.: *Kolloid Z. Z. Polymer*, 1962, vol. 181, pp. 131–137.
9. GLASSTONE, S., LAIDLER, K.J., and EYRING, H.: *Theory of the rate processes*, McGraw-Hill, New York, 1941, 611 pp.
10. EYRING, H.: *J. Chem. Phys.*, 1936, vol. 4, pp. 283–291.
11. EWELL, R., and EYRING, H.: *J. Chem. Phys.*, 1937, vol. 5, pp. 726–736.
12. BOCKRIS, J.O'M., and REDDY, A.K.N.: *Modern Electrochemistry*, Plenum Press, New York, 1970, vol. 1., 630 pp.
13. SEETHARAMAN, S., and DU SICHEN: *ISIJ Int.*, 1997, vol. 37, pp. 109–118.
14. NEMILOV, S.V.: *Fiz. Khim. Stekla*, 1978, vol. 4, pp. 129–148.
15. KINGERY, W.D., BOWEN, H.K., and UHLMANN, D.R.: *Introduction to ceramics*, 2nd edition, John Wiley & Sons, New York, 1976, 1032 pp.
16. MYSEN, B.O.: *Dev. Geochem.*, 1988, vol. 4, pp. 1–354.
17. WASEDA, Y., and TOGURI, J.M.: *The structure and properties of oxide melts*, World Scientific, Singapore, 1998, 236 pp.
18. FINCHAM, J.B., and RICHARDSON, F.D.: *Proc. Royal Soc.*, 1954, vol. 223, pp. 40–62.
19. GAYE, H.,and WELFRINGER, J.: *2nd Int. Symp. Metal. Slags Fluxes*, TMS-AIME, Warrendale, PA, 1984, pp. 357–375.
20. GUGGENHEIM, E.A.: *Proc. Royal Soc.*, 1935, vol. 148, pp. 304–312.
21. BLANDER, M., and PELTON, A.D.: *2nd Int. Symp. Metal. Slags Fluxes*, TMS-AIME, Warrendale, PA, 1984, pp. 295–304.
22. BALE, C.W., PELTON, A.D., and THOMPSON, W.T.: Facility for the Analysis of Chemical Thermodynamics (F*A*C*T), Ecole Polytechnique, Montreal, Canada, 2002, (http:\\www.crct.polymtl.ca).
23. JAK, E. and HAYES, P.C.: *9th Austr. Coal Sci. Conf.*, Austr. Inst. Energy, Toukley, NSW, Australia, 2000, CD-ROM.
24. *Slag Atlas*, 2nd edition, Springer-Verlag, Dusseldorf, 1995.
25. URBAIN, G.: *J. Mater. Educ.*, 1985, vol. 7, pp. 1007–1078.
26. URBAIN, G., BOTTINGA, Y., and RICHET, P.: *Geochim. Cosmochim.* Acta, 1982, vol. 46, pp. 1061–1072.
27. KOZAKEVITCH, P.: *Rev. Metall.*, 1960, vol. 57, pp. 149-160.
28. CHARTRAND, P., and PELTON, A.D.: *Calphad*, 1999, vol. 23, pp. 219–230.
29. KONDRATIEV, A., and JAK, E.: *Metall. Mater. Trans.* B, 2001, vol. 32B, pp. 1015–1025.

30. ELYUTIN, V.P., KOSTIKOV, V.I., MITIN, B.C. and NAGIBIN, Y.A.: *Zh. Fiz. Khim.*, 1969, vol. 43, pp. 579–583.
31. LOPATIN, V.M., NIKITIN, Y.P., BARMIN, L.N. and BOBYLEV, I.B.: *Fiz. Khim. Issled. Metall. Protsessov*, 1975, vol. 3, pp. 63–66.
32. VATOLIN, N.A., VYATKIN, G.P., ZOLATAREVSKII, B.M., IZMAILOV, Y.G. and UKHOV, V.F.: *VINITI* 4190-77, 1977, pp. 1–17.
33. SHIRAISHI, Y. and SAITO, T.: *Nippon Kinzoku Gakkaishi*, 1965, vol. 29, pp. 614–622.
34. SAITO, T. and KAWAI, Y.: *Sci. Rep. Res. Inst. Tohoku Univ.* A, 1951, vol. 3, pp. 491–501.
35. VIDACAK, B., DU SICHEN, and SEETHARAMAN, S.: *Metall. Mater.* Trans. B, 2001, vol. 32B, pp. 679–684.
36. CHEN, J.. GREENBERG, S., and POEPPEL, R.B.: *ANL/FE-83-30*, 1984, pp. 1–22.
37. SHELUDYAKOV, L.N., NURKEEV, S.S., IZOTOVA, E.T., KOSPANOV, M.M., and SABITOV, A.R.: *Kompleksn. Ispol. Miner. Syr'ya*, 1983, pp. 62–65.
38. BOCKRIS, J.O'M. and LOWE, D.C.: *Proc. Royal Soc.*, 1954, vol. A226, pp. 423–435.
39. URBAIN, G.: *Rev. Int. Haut. Temp. Refract.*, 1982, vol. 19, pp. 55–57.
40. SHIRAISHI, Y., IKEDA, K., TAMURA, A. and SAITO, T.: *Trans. Jap. Inst. Met.*, 1978, vol. 19, pp. 264–274.
41. KOZAKEVITCH, P.: *Rev. Metall.*, 1949, vol. 46, pp. 505–516, 572–582.
42. KUCHARSKI, M., STUBINA, N.M. and TOGURI, J.M.: *Can. Metall. Q.*, 1989, vol. 28, pp. 7–11.
43. KAIURA, G.H., TOGURI, J.M. and MARCHANT, G.: *Can. Metall. Q.*, 1977, vol. 16, pp. 156–160.
44. ROENTGEN, P., WINTERHAGER and H., KAMMEL, L.: *Z. Erz. u. Metal.*, 1956, vol. 9, pp. 207–214.
45. MYSLIVEC, T., WOZNIAK, J. and CERNY, V.: *Sb. Ved. Pr. Vys. Sk. Banaske Ostrave*, 1974, vol. 20, pp. 57–67.
46. MILLS, K.C., CHAPMAN, L., FOX, A.B. and SRIDHAR, S.: *6th Int. Conf. Slags Fluxes Molt. Salts*, 2000, KTH, Stockholm, CD-ROM, paper #433.
47. BLOMQUIST, R.A., FINK, J.K. and LEIBOWITZ, L.: *Ceram. Bull.*, 1978, vol. 5, p. 522.
48. HOFMAIER, G.: *Berg und Huttenm. Monatsh. Montan.* Hochschule Loeben, 1968, vol. 113, pp. 270–281.
49. SCHENCK, H., FROHBERG, M.G. and ROHDE, W.: *Archiv Eisenhuttenwes.*, 1961, vol. 32, pp. 521–523.
50. BACON, J.F., HASAPIS, A.A. and WHOLLEY, J.W.Jr.: *Phys. Chem. Glasses*, 1960, vol. 1, pp. 90–98.
51. HOFMAIER, G. and URBAIN, G.: *Sci. Ceram.*, 1968, vol. 4, pp. 25–32.
52. BOCKRIS, J.O'M., MACKENZIE, J.D. and KITCHENER, J.A.: *Trans. Faraday Soc.*, 1955, vol. 51, pp. 1734–1748.
53. BOWEN, D.W. and TAYLOR, R.W.: *Ceram. Bull.*, 1978, vol. 57, pp. 818–819.
54. ROSSIN, R., BERSAN, J. and URBAIN, G.: *Rev. Int. Haut. Temp. Refract.*, 1964, vol. 1, pp. 159–170.
55. BRUCKNER, R.: *Glastech. Ber.*, 1964, vol. 37, pp. 413–425.
56. LICKO, T. and DANEK, V.: *Phys. Chem. Glasses*, 1986, vol. 27, pp. 22–26.
57. URBAIN, G.: *Compt. Rendus*, 1951, vol. 232, pp. 330–332.
58. HURST, H.J., NOVAK, F. and PATTERSON, J.H.: *Fuel*, 1999, vol. 78, pp. 439–444.
59. HURST, H.J., PATTERSON, J.H. and QUINTANAR, A.: *Fuel*, 2000, vol. 79, pp. 1797–1799.
60. MACHIN, J.S. and YEE, T.B.: *J. Am. Ceram. Soc.*, 1948, vol. 31, pp. 200–204.
61. BILLS, P.M.: *J. Iron Steel Inst.*, 1963, vol. 201, pp. 133–140.
62. KATO, M. and MINOWA, S.: *Trans. ISI Japan*, 1969, vol. 9, pp. 31–38.
63. SCARFE, C.M., CRONIN, D.J., WENZEL, J.T. and KAUFFMAN, D.A.: *Am. Miner.*, 1983, vol. 68, pp. 1083–1088.